THE 4TH INTERNATIONAL CONFERENCE ON ALUMINUM ALLOYS

MICROSTRUCTURAL AND MICROMECHANICAL INFLUENCES ON FATIGUE CRACK PATH BEHAVIOUR IN Al-Li ALLOY AA8090

I. Sinclair and P.J. Gregson
Dept. of Engineering Materials, University of Southampton, Southampton, U.K.

Abstract

Factors controlling both microscopic and macroscopic fatigue crack growth characteristics in damage tolerant Al-Li based plate material have been investigated in relation to crack propagation mechanisms, grain size and the preferred orientation of {111} slip planes associated with the underlying crystallographic texture. Attention is paid to the phenomenon of macroscopic crack deviation observed in this material under certain testing conditions. The particular significance of crystallographic texture in determining macroscopic crack path behaviour is considered in relation to the crack tip micromechanics and the preferred orientation of {111} slip planes.

Introduction

Al-Li based alloys have attracted considerable interest as high specific strength/stiffness replacements for conventional high strength aluminium alloys used in the aerospace industry. It has also been noted that Al-Li materials may offer significant improvements in fatigue crack growth resistance over conventional high strength aluminium materials as a result of tortuous, slip-band (or 'Stage I'-type [1]) crack propagation and associated crack shielding mechanisms [2]. The incidence of slip-band crack growth in Al-Li alloys, *per se*, has been widely discussed in the literature and has been rationalised in terms of the heterogeneous, planar deformation mode often seen in these materials. Such deformation has been related to; (i) the presence of shearable δ' (Al_3Li) precipitates, promoting localised work-softening within slip-bands [3], and (ii) the strong crystallographic texture often developed in commercial Al-Li alloys, promoting the effective extension of slip-bands across grain boundaries of low angular misorientation [4].

Recent investigations into fatigue crack growth behaviour in commercial Al-Li plate materials in the damage tolerant condition have noted that, under certain conditions, sustained Stage I-type crack propagation may give rise to macroscopic crack deviation from a nominal mode I path during conventional fatigue testing [5,6]. It has been shown that whilst macroscopic deviation is intimately linked to slip band crack growth along a given preferred {111} plane orientation within a material (associated with the crystallographic texture), crack propagation during deviation requires a significant degree of co-planar, non-Stage I propagation in grains exhibiting different orientation variants of the overall texture [5]. The incidence of macroscopically deviated crack growth raises a number of important questions regarding the use of conventional structure lifing and fatigue testing methods with these materials. Whilst numerous investigations of fatigue crack growth in Al-Li materials have been presented in the literature, relatively little work has been carried out to clearly separate the influences of grain size, texture and specimen orientation on the incidence of Stage I crack propagation and associated crack path behaviour. In the present investigation, fatigue crack growth characteristics are reported for a number of commercial Al-Li

materials offering reasonably systematic variations in grain size and crystallographic texture. Crack growth has been examined in relation to test orientation and resultant microscopic and macroscopic crack path behaviour.

Experimental

Materials Two batches of the commercial Al-Li-Cu-Mg alloy AA8090 in the damage tolerant T8151 condition were utilised: (i) Plate A, produced in 28mm thick form, and (ii) Plate B, produced in 12.5mm thick form. It is noted that whilst the full as fabricated thickness of Plate A was supplied for investigation, only material from the central 5mm of Plate B was available. Longitudinal and transverse room temperature tensile properties at a strain rate of 5×10^{-4} s^{-1} were obtained for both materials at the t/2 position, and for Plate A at the t/6 position using ~1.5mm thick, flat 'dogbone'-type tensile specimens (30mm gauge length), see Table I.

Table I Monotonic tensile properties of AA8090-T8151 Plate

Material	Through-Thickness Position	Orientation	Yield Stress (MPa)	UTS (MPa)	% Elongn.
Plate A	t/2	L	414	475	3.6
		T	389	479	6.0
	t/6	L	356	451	7.5
		T	317	448	10.7
Plate B	t/2	L	421	485	3.7
		T	405	484	6.7

An elongated pancake grain structure was evident in both plate materials, with measured linear intercept dimensions as shown in Table II. It may be seen from this table that there was a marked decrease in grain size in Plate A between the t/2 and and t/6 regions (an approximate order of two variation), with the t/2 position grain dimensions in Plate B being relatively similar to the t/6 position in Plate A. Grain size was not seen to vary significantly with through-thickness position in the supplied form of Plate B, consistent with the prior machining down of this material. Conventional back-reflection X-ray diffraction measurements showed a predominant 'brass'-type texture (i.e. close to {110} <112>) at the t/2 through-thickness position for both Plates A and B, see Fig. 1 (a). Average maximum intensities for the four central orientation peaks in the t/2 position pole figures were noted as 9.1 and 9.7 times random for Plate A and B respectively. A marked change in texture was noted towards the plate surface in Plate A, with a predominant mixture of both 'copper' ({112}<111>) and 'S' ({123}<634>) deformation textures being observed at the t/5 position, see in Fig. 1 (b). Average peak intensities associated with the t/6 pole figure were 4.5 times random, i.e. somewhat lower than the t/2 peak measurements.

Table II Grain dimensions measured in AA8090-T8151 Plate.

	Grain Dimensions (μm)					
	t/2			t/6		
	L	T	S	L	T	S
Plate A	200	165	20	95	60	10
Plate B	90	55	9	-	-	-

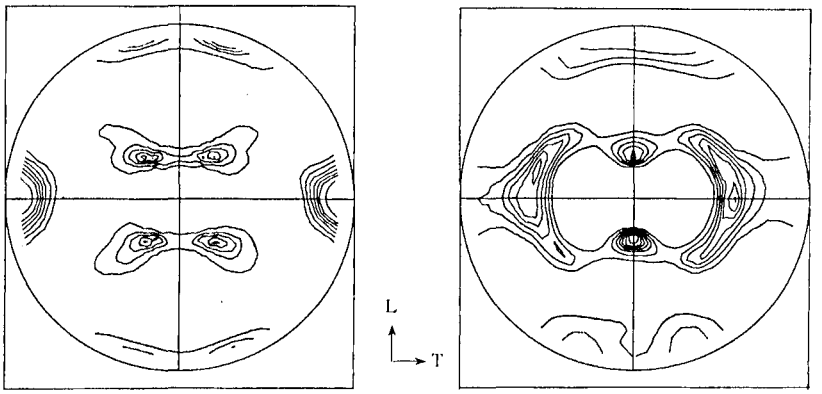

Figure 1 {111} Pole figures corresponding to Plate A: (a) t/2 position, contours levels at 1.0, 3.0, 5.0, 7.0, 9.0, 11.0, and (b) t/6 position, contour levels at 1.0, 1.6, 2.2, 2.8, 3.4, 4.0, 4.6.

Fatigue Testing A number of TL and LT orientation fatigue crack growth tests of Plate A and B were carried out using 5mm thick, 100mm wide centre cracked tension (CCT) specimens, as summarised in Table III.

Table III Fatigue Test Variables

Test No.	Material	Plate Position	Orientation
1	Plate A	t/2	TL
2	Plate B	t/2	TL
3	Plate A	t/6	TL
4	Plate A	t/2	LT

All tests were performed under constant cyclic load/increasing ΔK conditions using an automated electro-servo hydraulic testing machine in general accordance with British Standard BS 6835:1988 [7]. Testing was carried out at a frequency of 10Hz in laboratory air at an R-ratio of 0.1. Crack growth was monitored using a four-probe pulsed d.c.p.d method and was typically produced from just above the near-threshold regime (i.e. $da/dN \lesssim 10^{-6}$ mm/cycle) to failure.

Fractography In addition to standard optical and SEM fractographic techniques, etch pit studies were carried out to identify the crystallographic orientation of microscopic fracture surface features. Etch pitting was carried out using a 50 H_2O : 50 HNO_3 : 32 HCl : 2 HF mixture, as described by Bowles and Broek [8]. Typical etch pit characteristics are illustrated in Fig. 2.

Results

Macroscopic Behaviour Both TL orientation, t/2 CCT specimens (i.e. Test Nos. 1 and 2) exhibited pronounced macroscopic crack deviation, as illustrated in Fig. 3 (a & b). Deviation occurred through an angle of ~ 60° at a ΔK level of ~ 15 MPa$\sqrt{m}$ in both cases. Crack growth in these specimens exceeded the degree of out-of-plane deviation permitted by BS 6835:1988 beyond a nominal ΔK of ~ 17 MPa$\sqrt{m}$. The t/6, TL orientation Plate A specimen (Test No. 3) did not exhibit overall macroscopic deviation, as shown in Fig. 4 (a - c). A definite through-thickness variation in macroscopic crack behaviour was however evident above a ΔK of ~ 12 MPa$\sqrt{m}$, with one side of the specimen showing relatively flat crack growth up to monotonic failure, whilst the

other side showed distinct crack meandering (particularly for $\Delta K \gtrsim 16$ MPa$\sqrt{m}$), see Fig. 4 (b & c). Crack growth on the 'rough' side of this specimen just exceeded the degree of out-of-plane deviation permitted by BS 6835:1988 beyond a nominal ΔK of ~ 22 MPa$\sqrt{m}$. The LT orientation, t/2 Plate A specimen (Test No 4) showed no evidence of macroscopic deviation, with the overall crack path remaining within ± 0.5 mm of the nominal mode I crack growth plane up to monotonic failure.

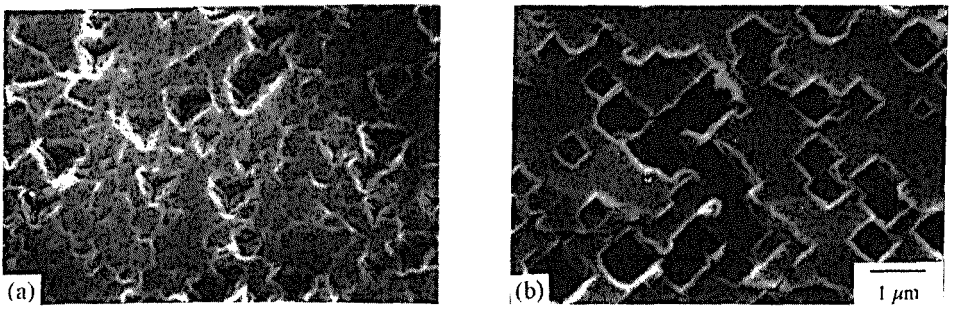

Figure 2 Typical etch pitting behaviour, (a) threefold symmetry associated with {111} plane orientations, and (b) fourfold symmetry associated with {001} plane orientations.

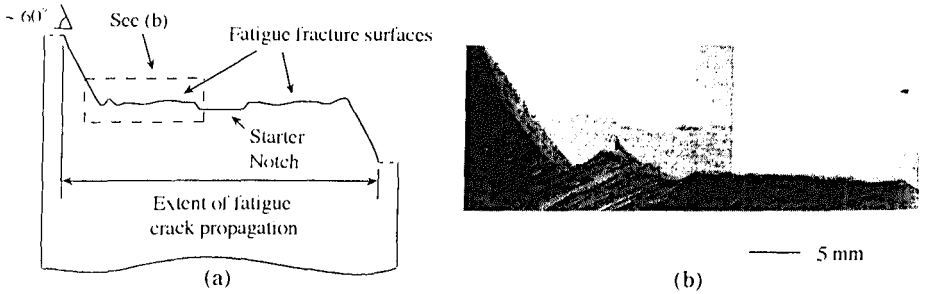

Figure 3 Macroscopic crack deviation behaviour observed in TL orientation, t/2 position specimens, (a) broken specimen schematic, and (b) fracture surface profile.

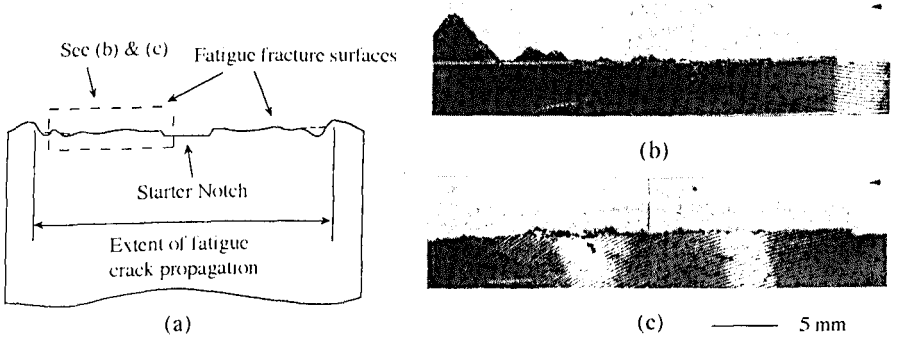

Figure 4 Macroscopic crack path behaviour observed in TL orientation, t/6 Plate A specimen, (a) broken specimen schematic, (b) & (c) opposing face fracture surface profiles.

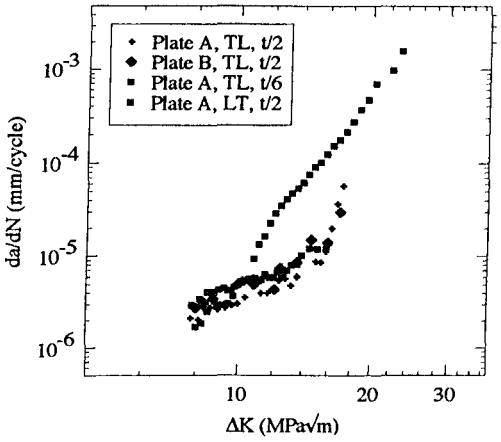

Fig. 5 Fatigue crack growth rates in 8090-T8151.

Macroscopic fatigue crack rates are shown in Fig. 5. It may be seen that over the range available for comparison, data from all of the TL orientation specimens (Tests 1 - 3) fell within the same general band covering an approximate factor of two variation in growth rates. Crack growth rates from the LT oriented, t/2 Plate A specimen are seen to be similar to the three TL orientation tests up to a ΔK of approximately 11 MPa$\sqrt{m}$, but are significantly higher than the TL orientation data at higher ΔK levels (by up to an order of magnitude).

Microscopic Behaviour At the lower ΔK levels investigated here ($\lesssim$ 11 MPa$\sqrt{m}$), a mixture of quite well defined blocky facets and comparatively less faceted areas was identified in all of the tests, see Fig. 6 (a). Etch pitting showed the well defined facets to be generally associated with crack growth close to {111}-type planes, whilst the less obviously crystallographic areas often showed near {001}, and occasionally {011} orientations. In all specimens the proportion of well defined faceted crack growth was seen to increase with increasing stress intensity, with faceting tending to predominate by a ΔK of approximately 12 MPa$\sqrt{m}$, see Fig. 6 (b). With further increases in ΔK levels the scale of tortuousity associated with faceted crack growth was seen to increase quite significantly in all of the specimens, see Fig. 6 (c) & (d), this being particularly clear in specimens showing macroscopic deviation, as such crack growth was clearly associated with a particularly sustained, flat faceted growth mode in the macroscopic growth direction, see Fig 6 (c). Etch pitting showed that during macroscopic deviation extensive {111} oriented crack growth had occurred, although a large proportion of co-planar facets exhibiting irregular and occasionally {001}-type pitting were also noted. A similar combination of crystallography was identified on microstructurally large facets in the other test specimens (i.e. those at higher ΔK levels in the LT orientation and on the 'rough' side of the t/6 Plate A specimen particularly). Sectioning of the t/2 plate position test specimens (i.e. those exhibiting a brass-type texture) showed that in all three cases the orientation of faceted crack growth at higher ΔK levels was consistent with the four central orientation peaks associated with the {111} pole figure shown in Fig. 1 (a).

Discussion

Various factors may be identified as potentially influencing the incidence of slip band crack propagation in an Al-Li material, e.g. (i) precipitate condition, influencing the intrinsic propensity for inhomogeneous deformation, (ii) grain size, influencing the scale over which the deformation homogenising effect of grain boundaries may operate, (iii) crystallographic texture, influencing the statistical distribution of grain boundary misorientations and the orientation of available slip systems in relation to the crack tip stress/strain fields, and (iv) environmental interactions, which may promote specific crack growth mechanisms through the up-take of hydrogen from water vapour. In the absence of detailed quantitative analysis, it would appear that the change in crack growth mechanism observed with increasing stress intensity levels was similar for all of the tests reported here (i.e. the shift towards slip-band dominated propagation occurring over similar stress

intensity levels in each case). Resent studies by Piascik and Gangloff [9] have indicated that the occurrence of {001} and {011} oriented crack growth in various commercial Al-Li materials at low growth rates is directly related to environmental interactions, with slip-band dominated crack growth occurring at all growth rates in these materials when tested in vacuum. The results obtained here are consistent with an environmentally dominated control of crack growth mechanism, with the various changes in microstructure and test orientation considered having relatively little effect on the increased incidence of faceted crack growth with increasing ΔK levels.

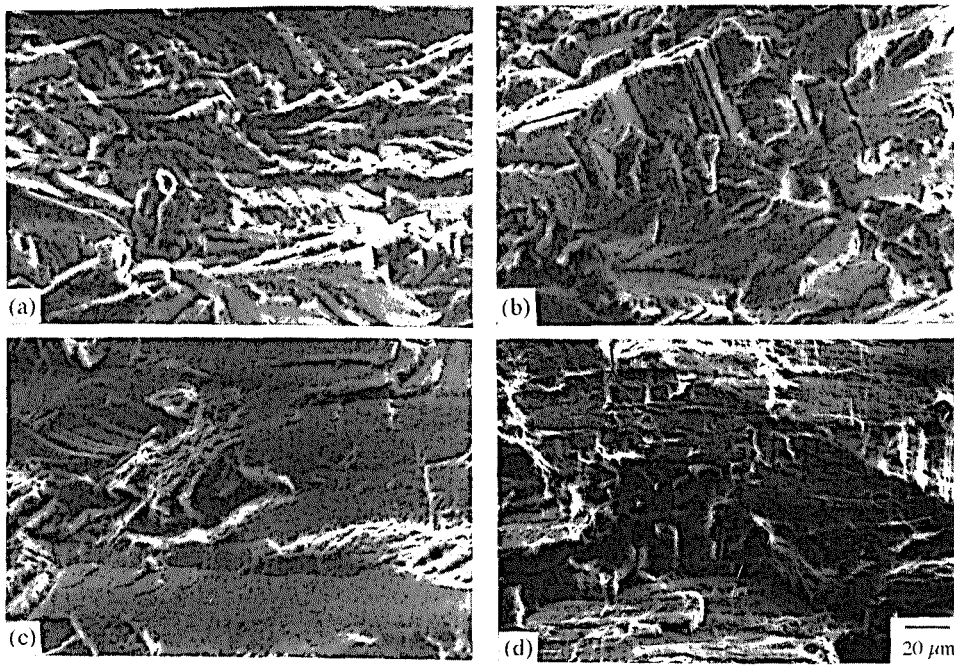

Figure 6 Fatigue fracture surfaces in Plate A, TL, t/2 specimen at: (a) $\Delta K \sim 9$ MPa$\sqrt{m}$, (b) $\Delta K \sim$ 13 MPa$\sqrt{m}$, (c) post macroscopic deviation, and (d) LT, t/2 specimen, $\Delta K \sim 20$ MPa$\sqrt{m}$.

Whilst there there was a strong propensity for slip-band crack propagation to occur at higher ΔK levels in all of the tests reported here, it was clear that marked changes in overall crack path behaviour were produced by variations in specimen orientation and underlying crystallographic texture, although crack path appeared to be relatively insensitive to changes in grain size. In terms of the conventional wisdom concerning crack path meandering during Stage I-type crack propagation, it is generally suggested that changes in crack growth direction occur as grains of different orientations present different {111} plane orientations on which propagation can occur [10]. The brass-type texture is made up of two equivalent orientation variants, as illustrated in Fig. 7 in relation to a nominal TL orientation crack. The planes which are angled to the through-thickness direction in each case contribute to the four central orientation peaks seen in the {111} pole figure in Fig. 1 (a). As noted in a previous paper [5], the particularly flat, co-planar crack propagation associated with macroscopic deviation in the TL orientation t/2 test specimens was associated with {111} oriented crack growth on the through-thickness angled planes of one of the texture variants, with co-planar, but non-{111} oriented propagation occurring in grains of the other possible orientation. In this context it is interesting to note the recent work of Xu *et al.* [11],

who have noted that co-planar deformation bands may propagate between {111} orientation and other, high index planes in adjacent grains in commercial Al-Li materials. It is clear that such behaviour may well be related to the mixed crystallography, co-planar crack propagation behaviour seen in the current work.

In terms of the orientation effect on crack path behaviour in the brass texture materials, it is clear that changes in the actual crack growth mechanism do not rationalise the results obtained here, as crack growth at higher ΔK levels in both the TL and LT orientation occurred by the same micromechanisms on microstructurally identical planes. It is however valuable to consider the crack tip stress intensity conditions associated with locally deviating crack paths. Fig. 8 shows how, for a simply kinked crack in two dimensions, the local ratio of mode I and II stress intensities vary with kink angle, θ, under purely elastic conditions [12]. It may be seen that the proportion of mode II crack opening increases dramatically with θ. In the LT orientation crack growth was associated with a kink angle of ~35°, whilst in the TL orientation the corresponding angle was ~55°. Given that mode II loading promotes a strong co-planar stress/strain concentration ahead of a crack, it may be seen that an increasing proportion of mode II acting at a crack tip may particular promote sustained co-planar Stage I-type crack propagation. Recent mixed mode fatigue testing by the authors has shown that mode II loading of a crack parallel to a preferred {111} plane orientation will in fact produce macroscopically sustained co-planar crack propagation in these materials [13]. Whilst the purely elastic results shown in Fig. 8 may not be wholely representitve of the local elastic-plastic conditions at relatively small kink sizes, it may be seen that a higher mode II loading component experienced by a 55° kink, as opposed to a 35° kink, may be used to rationalise the incidence of sustained co-planar kink formation (i.e. macroscopic deviation) in the TL test orientation, but not in the LT. It should be noted that the crack paths observed in TL and LT oriented t/2 materials were both kinked *and* twisted with respect to the nominal mode I crack planes, and a full analysis of local crack tip conditions during crack deviation would clearly require some consideration of mode III loading effects. In the first instance it may be noted that the change in twist angle associated with faceted crack growth in the TL and LT specimen orientations (~65 and 55° respectively, in relation to the through-thickness direction) is somewhat less than the associated changes in kink angle, and may therefore be expected to be less critical in differentiating crack growth behaviour in the two test orientations.

Given a limited grain size effect on fatigue crack propagation behaviour in the plate mid-thickness materials, the observed differences between the t/6 and t/2, TL oriented Plate A test specimens, and the through-thickness variation in behaviour across the t/6 specimen, may be primarily attributed to variations in underlying crystallographic texture. In general, terms the available texture information would appear to be consistent with crack path behaviour in the t/6 test specimen, in that the increased number of ideal grain orientations on going from the centre to the surface of the plate (the brass textures consisting of two variants, as opposed to two and four variants for the S and copper textures respectively) and generally reduced intensity of texture would; (i) be expected to prevent a specific {111} plane from dominating deformation/crack path behaviour, and (ii) reduce the proportion of grains suitably oriented for strong local mode II loading during crack kinking.

Conclusions

1. The prevalence of {111} oriented crack propagation in Al-Li alloys has been confirmed, with the incidence of {001} and occasionally {011} oriented propagation at lower stress intensity levels being noted and attributed primarily to environmental interactions.

2. The incidence of macroscopic crack deviation has been shown to be directly related to specimen

orientation, the presence of a strong, brass-type crystallographic texture, and relatively insensitive to changes in grain size.

3. The scale of crack path meandering set-up during Stage I-type crack propagation has been related to the orientation of {111} slip planes, crack path kinking geometry and local mixed mode crack tip loading conditions.

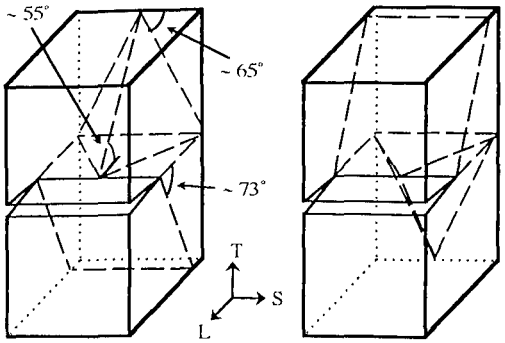

Fig. 7 Schematic illustration of spatial relationship between a TL oriented crack and peak preferred {111} plane orientations associated with a brass type texture

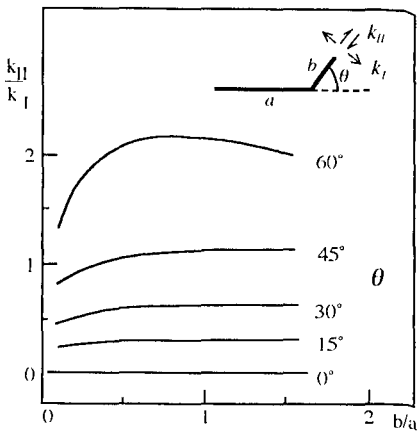

Figure 8 Variation in local mixed mode loading condition associated with crack kinking

Acknowledgements

Financial support of this research was provided by British Aerospace, Airbus Division (Filton, UK). The help of Dr A.W. Bowen (DRA, Farnborough, UK) is gratefully acknowledged.

References

[1] Forsyth, P.J., in *Crack Propagation*, (1961), Proc. Cranfield Symp., London: HMSO, 76.

[2] Venkateswara Rao, K.T. and Ritchie, R.O., (1992), *Int Met Rev*, **37**, 341.

[3] Sanders, T.H. and Starke, E.A., *Acta Metall.*, **30**, (1982), 927-939.

[4] Gregson, P.J. and Flower, H.M., (1985), **33**, 527.

[5] Sinclair, I. and Gregson, P.J., (1993), in *Fatigue 93*, Proc. 5th Intl.Conf. of Fatigue and Fatigue Thresholds, eds. Baïlon, J-P. and Dickson, J.I., Warley: MCEP, Vol. 2, 635.

[6] Sinclair, I. and Gregson, P.J., (1993), Report No. EMR 38/10/93, University of Southampton, UK.

[7] *Determination of the Rate of Fatigue Crack Growth in Metallic Materials*, British Standard BS6835:1988, (1988), Milton Keynes: British Standards Institution.

[8] Bowles, C.Q. and Broek, D., (1972), *Int. J. Frac. Mech.*, **8**, 75.

[9] Piascik, R.P. and Gangloff, R.P., (1993), *Met. Trans. A*, **24A**, 2751.

[10] Suresh, S., (1991), in *Fatigue of Materials*, Cambridge: CUP.

[11] Xu, Y.B., Wang, L., Zhang, Y., Wang, Z.G. and Hu, Q.Z., (1991), *Met. Trans. A*, **22A**, 723.

[12] Suresh, S., (1983), *Met. Trans. A*, **14A**, 2375.

[13] Sinclair, I. and Gregson, P.J., (1994), *Scripta Met. Mater.*, **30**, 1287.